Spot spectroscopy of highly ionized europium

J. Bailey
Sandia National Laboratory, Albuquerque, New Mexico 87185

J. D. Kilkenny, Y. Lee, S. Maxon, J. H. Scofield, and D. Weber
Lawrence Livermore National Laboratory, University of California, Livermore, California 94550
(Received 14 November 1986)

Microdot spectroscopy of a laser-produced plasma was used to study the x-ray emission from highly ionized europium in the wavelength region between 6.5 and 9.6 Å. New identifications of spectral lines from europium ions isoelectronic with Ni, Co, and Fe were made using *ab initio* calculations of the wavelengths and gf values. The emission was measured with spatial and temporal resolution and as a function of the laser irradiance. The relative abundances of the different ionization stages, as inferred from the intensities of the $3d$-$4f$ transitions, compare favorably with the ionization distribution predicted by a collisional-radiative model and with the results of a two-dimensional LASNEX simulation.

I. INTRODUCTION

Laser-produced plasmas have proved to be valuable sources for studying the spectroscopy of high-Z ions. To date, such studies have concentrated on identification of Ni-like transitions.[1-6] The shapes of the spectra have also been interpreted[7,8] in terms of unresolved transition arrays. In this paper we report experimental results from highly ionized europium ($Z=63$). New identifications were made with use of *ab initio* calculations of the wavelengths and the gf values for 60 $n=4$ to $n=3$ transitions (n is the principal quantum number) in europium ions isoelectronic with Ni, Co, and Fe. The relative abundance of the ionization stages as a function of laser irradiance was determined qualitatively by comparing the intensities of the $3d$-$4f$ transitions. The predictions of a two-dimensional LASNEX simulation and a collisional-radiative model are in reasonable agreement with these relative abundances. The data indicate that to determine the ionization distribution from the $3d$-$4f$ transitions, we must consider the detailed structure of the spectra instead of using the unresolved arrays.

II. EXPERIMENTAL CONDITIONS

Microdot spectroscopy[9,10] was used to form a plasma column with small source size, low opacity, and one-dimensional temperature and density gradients. The dot material was 98 at.% Al + 2 at.% Eu with a 1000-Å NaCl overcoat, vacuum evaporated onto a Mylar substrate. The dot was 5000 Å thick and the diameter was 25 μm. The Janus laser facility at Lawrence Livermore National Laboratory was used to irradiate the target with 0.53-μm light in a 1-nsec pulse. The irradiance was varied from 6×10^{13} to 2×10^{14} W/cm^2.

The principal diagnostics were a spatially resolved, time-integrated ammonia dihydrogen phosphate (ADP) flat-crystal spectrometer and a spatially integrated, time-resolved potassium acid phthalate (KAP) flat-crystal streaked spectrometer. Both spectrometers viewed the plasma column at approximately 90°. The space-resolving spectrometer was equipped with two slits, 30 μm and 80 μm wide, which were perpendicular to the axis of the plasma column. The magnification was about four, so that the spatial resolution was 38 μm and 100 μm, respectively, for the two slits. The streaked spectrometer viewed the entire plasma and had a time resolution of 200 psec. An x-ray pinhole camera filtered to observe energies greater than 1 keV was also used to monitor the size of the plasma column.

III. RESULTS

Tracings of europium spectra obtained with the space-resolving spectrometer are shown in Fig. 1. Figure 1(a) is from a high-irradiance shot; the tracing is an average over 30 μm in the plasma, located adjacent to the target surface. Figure 1(b) is a comparison between high- and low-irradiance shots for wavelengths between 8.0 and 9.4 Å. The low-irradiance shot had a lower signal level, forcing us to average over 100 μm of the plasma column (for both the low- and high-irradiance shots) in Fig. 1(b). The spectra were corrected for the response of the Kodak DEF-5 film,[11] the crystal reflectivity,[12] the filter transmission, and geometrical factors.

The prominent bands of europium transitions visible in the high-irradiance shot are due to $3d$-$4f$ transitions from Eu ions isoelectronic with $_{28}$Ni, $_{27}$Co, $_{26}$Fe, Mn, and Cr. The emission from Mn-like and Cr-like europium is not present in the spectrum from the low-irradiance shot. Other lines observed in these spectra were Al He$_\alpha$, Al Ly-α, Al He$_\beta$, and Na Ly-α. These lines were used as the primary wavelength standards.

The identifications of Ni-like lines are listed in Table I. The calculated values are the results of a relativistic configuration-interaction calculation which includes the Breit magnetic and retardation interaction in the long-wavelength limit. The single-particle wave functions used

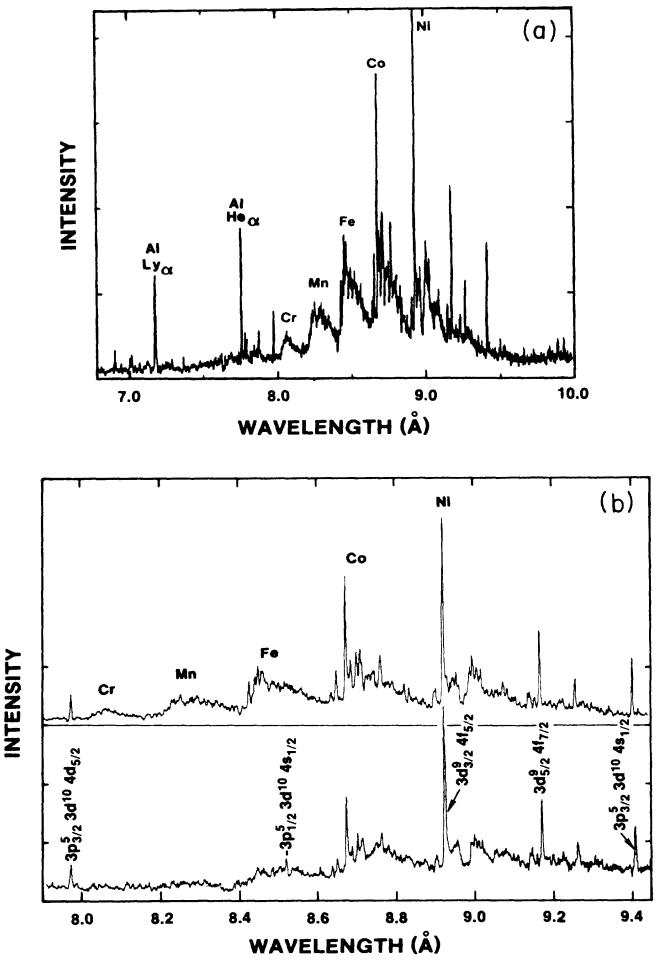

FIG. 1. Spatially resolved, time-integrated, single-shot spectra from europium. In (a) the laser irradiance was 2×10^{14} W/cm^2. The $3d$-$4f$ europium transition arrays are labeled according to the ionization stage. In (b) a portion of this spectrum (top) is compared with the spectrum obtained from a shot at 6×10^{13} W/cm^2 (bottom). The labeled lines are from Ni-like transitions with the indicated upper state (the ground configuration is $3p^63d^{10}$).

in the expansion of the states were generated by an average-configuration relativistic Hartree-Fock calculation.[13] The calculations were carried out including all couplings of states with a given number of $n=3$ and $n=4$ electrons of a fixed angular momentum and parity. The radiative gf values were calculated using the relativistic-length form of the electric dipole interaction which includes the effects of retardation. The theoretical wavelengths had to be shifted upward by 23 mÅ to obtain the optimum agreement with the experimental values. The average difference between the theoretical and experimental values is ±4 mÅ. The expected experimental accuracy of the absolute wavelengths is better than ±10 mÅ and the accuracy of the relative spacings is approximately ±2 mÅ. The utility of comparing different laser intensities is demonstrated by the identification of the $3p^5_{1/2}3d^{10}4s_{1/2}$ feature at 8.520 Å. This line, which overlaps the Fe-like $3d$-$4f$ transition array, is indistinguishable in the high-irradiance spectrum and quite prominent in the low-irradiance spectrum.

Individual Co-like and Fe-like lines have also been identified. The spectral regions for these transitions are shown on an expanded scale in Figs. 2 and 3, respectively, with the theoretical gf values superimposed on the experimental data. These tracings represent an average over 30 μm in the plasma column, located next to the target surface. The line identifications are listed in Tables II and III. The Co-like upper states in Table II are listed in j-j coupling with the notation $(3l_{1j_1}3l_{2j_2})\,J_a4l_{j_3}J'$. The electrons $3l_{1j_1}$ and $3l_{2j_2}$ couple into J_a, which couples with the $4l_{j_3}$ electron to obtain J', the total angular momentum for the upper state. The Fe-like upper states in Table III are also listed in j-j coupling. The notation $[(3d^r_{3/2})_s(3d^t_{5/2})_u]_v4f_wJ'$ means that the r electrons in $3d_{3/2}$ couple into $j=s$, the t electrons in $3d_{5/2}$ couple into $j=u$, s couples with u into $j=v$, and v couples with the $4f_w$ electron to obtain J'. The experimental intensities in Table II refer to the line intensity above the broad quasicontinuum hump. The average difference between the theoretical wavelength predictions and the measured values is ±5 mÅ.

In previous studies[3] of other elements the line equivalent to the bright feature at 9.264 Å was attributed

TABLE I. Identifications of Ni-like europium. The theoretical wavelengths are shifted upward by 23 mÅ. The experimental intensities are from the tracing of the high-irradiance shot shown in Fig. 1(a) (average over 30 μm of plasma) and are scaled so that the strongest line agrees with its gf. The ground configuration is $3p^63d^{10}$.

Wavelength (Å)		Intensity		
Experiment	Theory	Experiment	gf	Upper level
9.410	9.401	1.56	0.38	$3p^5_{3/2}3d^{10}4s_{1/2}$
9.173	9.184	2.00	1.03	$3d^9_{5/2}4f_{7/2}$
8.925	8.921	6.30	6.30	$3d^9_{3/2}4f_{5/2}$
8.520	8.515		0.043	$3p^5_{1/2}3d^{10}4s_{1/2}$
7.972	7.975	0.76	1.03	$3p^5_{3/2}3d^{10}4d_{5/2}$
7.363	7.367	0.30	0.50	$3p^5_{1/2}3d^{10}4d_{3/2}$
7.246	7.244		0.035	$3s_{1/2}3p^63d^{10}4p_{1/2}$
7.066	7.065	0.24	0.14	$3s_{1/2}3p^63d^{10}4p_{3/2}$

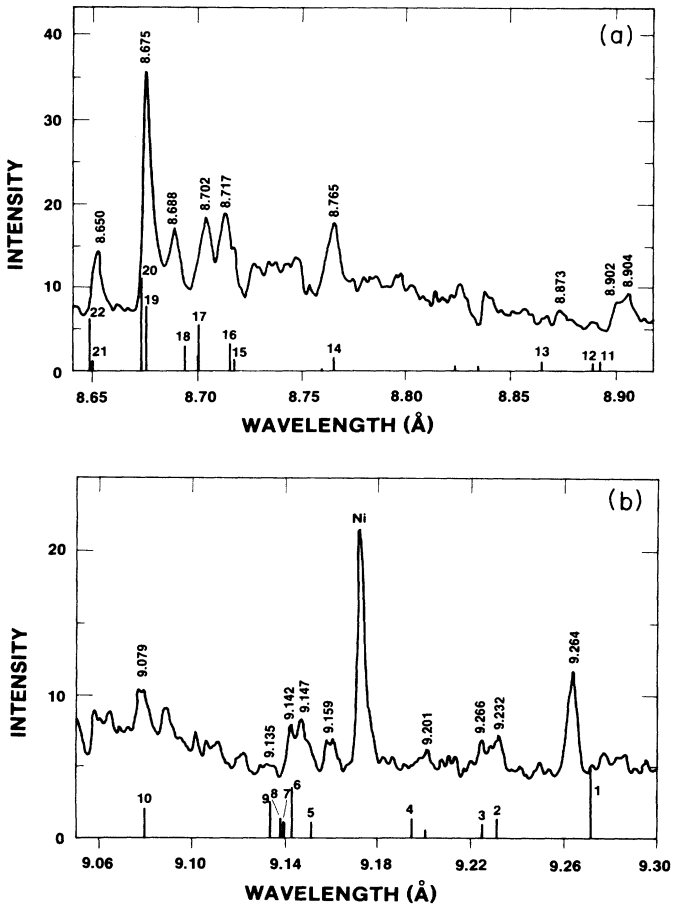

FIG. 2. Portions of the spectrum obtained on the high-irradiance shot, shown on an expanded scale. The line numbers correspond to Table II. (a) shows the Co-like $3d$-$4f$ transitions and (b) shows the $3p$-$4s$ transitions.

to the Ni-like $3p^6 3d^{10}$-$3p^6 3d^9_{5/2} 4f_{5/2}$ transition. We have identified this line as a $3p$-$4s$ Co-like transition from the $(3p_{3/2} 3d_{5/2})_{J=4} 4s_{1/2} (J'=3.5)$ level. This identification is based on three facts. First, the theoretical wavelength for the Ni-like $3p^6 3d^9_{5/2} 4f_{5/2}$ transition is 9.298 Å, 34 mÅ from the experimental feature (compared to an average discrepancy of ±4 mÅ for the other Ni-like lines). Second, the gf for the $3d^9_{5/2} 4f_{5/2}$ transition is a factor of 400 lower than the gf for the $3d^9_{3/2} 4f_{5/2}$ transition, while the experimental intensity ratio is about 6.6 (Tables I and II). The discrepancy between the gf's and the experimental intensities for the other Ni-like lines is ±50%. Finally, the other $3p$-$4s$ Co-like lines are clearly present, with the relative spacings and intensity ratios in good agreement with the experimental spectrum [Fig. 2(b) and Table II].

Tracings from a spatially integrated streaked spectrum are shown in Fig. 4. The intensities have been corrected for the response of the Kodak Royal X-Pan film. The laser intensity was 8×10^{13} W/cm^2 on this shot. The spectral resolution was sufficient to resolve the $3d$-$4f$ transition arrays from different ionization stages, but not the individual europium lines. The relative strength of

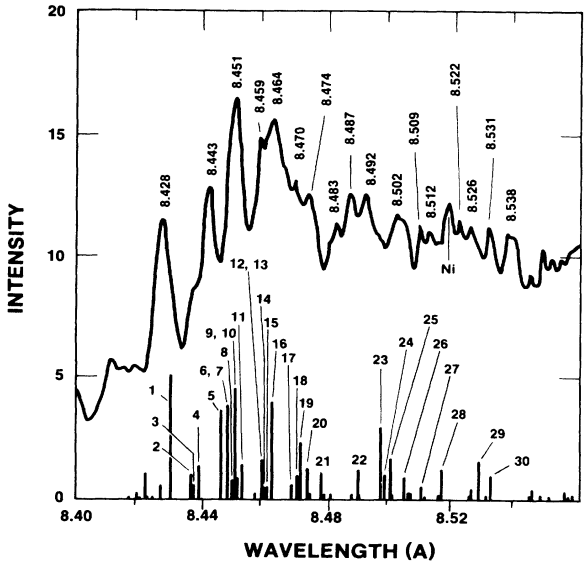

FIG. 3. Portion of the high-irradiance spectrum showing the Fe-like $3d$-$4f$ transitions. The line numbers correspond to Table III.

the radiation from the different ionization stages changes on a time scale equal to or less than the time resolution of the streak camera (200 psec). The total duration of the europium radiation is comparable to the laser pulse length, in contrast to the Al XII and Al XIII resonance lines which last about twice as long.

IV. DISCUSSION AND CONCLUSIONS

It is not possible to rigorously determine the relative abundances of the ionization stages from the $3d$-$4f$ emission without detailed information on the population mechanisms for the excited states. As a zero-order approximation, we have compared the ionization abundances inferred from the relative intensities of the $3d$-$4f$ emission with the ionization distribution predicted by a collisional-radiative (CR) model and by a separate two-dimensional LASNEX simulation. The first problem we encounter in applying this method is that the $3d$-$4f$ radiation from ions stripped higher than Ni-like consists of a broad hump with sharp peaks superimposed on it. This is true even though the spectral resolution achieved by using the microdot technique was higher ($\lambda/\Delta\lambda\sim3000$) than in previous work. In measuring the experimental intensities, it is not certain whether the contribution from the hump should be included, since its origin is unknown.

There are indications from previous work that the hump is due to satellite transitions from lower ionization stages. Burkhalter *et al.*[1] observed that the quasicontinuum hump in a gadolinium spectrum "tails" toward the low-energy side of the resonance lines and they suggested that this was due to satellite transitions with a spectator electron in the $4l$ subshell. In addition, the relative intensity of the humps and the superimposed peaks varies as we would expect if the hump were due to satellite transitions [Refs. 1—6 and Fig. 1(c)]. That is, in a colder plas-

TABLE II. Identifications of Co-like europium. The theoretical wavelengths were shifted upward by 23 mÅ for the $3p$-$4s$ transitions and 20 mÅ for the $3d$-$4f$ transitions. The upper levels are listed in j-j coupling. The experimental intensities are from the high-irradiance shot shown in Fig. 1(a) (average over 30 μm of plasma) and are scaled relative to the strongest Ni-like line, as in Table I.

Line No.	Wavelength Expt.	Wavelength Theory	Expt. intensity	gf	Upper level			J'	J
1	9.264	9.273	0.95	0.80	$(3p_{3/2}3d_{5/2})$	$J=4$	$4s_{1/2}$	3.5	2.5
2	9.232	9.233	0.57	0.22	$(3p_{3/2}3d_{5/2})$	$J=2$	$4s_{1/2}$	2.5	2.5
3	9.226	9.227	0.32	0.16	$(3p_{3/2}3d_{5/2})$	$J=2$	$4s_{1/2}$	1.5	2.5
4	9.201	9.196	0.26	0.24	$(3p_{3/2}3d_{3/2})$	$J=2$	$4s_{1/2}$	1.5	1.5
5	9.159	9.153	0.46	0.18	$(3p_{3/2}3d_{5/2})$	$J=3$	$4s_{1/2}$	3.5	2.5
6	9.147	9.155	0.76	0.58	$(3p_{3/2}3d_{3/2})$	$J=3$	$4s_{1/2}$	2.5	1.5
7	9.142	9.142	0.37	0.20	$(3p_{3/2}3d_{3/2})$	$J=1$	$4s_{1/2}$	1.5	1.5
8		9.141		0.22	$(3p_{3/2}3d_{3/2})$	$J=2$	$4s_{1/2}$	0.5	1.5
9	9.135	9.136		0.41	$(3p_{3/2}3d_{5/2})$	$J=3$	$4s_{1/2}$	2.5	2.5
10	9.079	9.081	0.43	0.33	$(3p_{3/2}3d_{5/2})$	$J=1$	$4s_{1/2}$	1.5	2.5
11	8.904	8.915	1.1	1.5	$(3d_{3/2}3d_{5/2})$	$J=4$	$4f_{7/2}$	2.5	1.5
12	8.902	8.912		1.1	$(3d_{3/2}3d_{5/2})$	$J=4$	$4f_{7/2}$	1.5	1.5
13	8.873	8.885	0.35	1.3	$(3d_{3/2}3d_{5/2})$	$J=3$	$4f_{7/2}$	0.5	1.5
14	8.765	8.777	2.0	2.2	$(3d_{3/2}3d_{3/2})$	$J=0$	$4f_{5/2}$	0.5	1.5
15	8.717	8.725	2.2	2.0	$(3d_{3/2}3d_{5/2})$	$J=4$	$4f_{7/2}$	1.5	2.5
16		8.723		4.4	$(3d_{3/2}3d_{3/2})$	$J=2$	$4f_{5/2}$	2.5	1.5
17	8.702	8.707	1.7	7.2	$(3d_{3/2}3d_{3/2})$	$J=2$	$4f_{5/2}$	1.5	1.5
18	8.688	8.700	1.4	3.9	$(3d_{3/2}3d_{5/2})$	$J=4$	$4f_{5/2}$	1.5	2.5
19	8.675	8.679	5.2	10.9	$(3d_{3/2}3d_{5/2})$	$J=4$	$4f_{5/2}$	2.5	2.5
20		8.677		15.0	$(3d_{3/2}3d_{5/2})$	$J=1$	$4f_{5/2}$	3.5	2.5
21	8.650	8.650	1.3	8.4	$(3d_{3/2}3d_{3/2})$	$J=0$	$4f_{5/2}$	2.5	1.5
22		8.650		1.6	$(3d_{3/2}3d_{3/2})$	$J=2$	$4f_{5/2}$	3.5	2.5

ma (lower laser intensity) the hump is relatively more intense and as the target atomic number is increased the hump becomes brighter compared to the peaks. A theoretical spectrum obtained by assigning a Gaussian shape (with the experimentally determined instrumental width) to the lines does not reproduce the quasicontinuum hump under the peaks. However, Busquet *et al.*[6] were successful in reproducing an experimental Au spectrum using an empirically formulated synthetic spectrum consisting of lines with a red wing added.

The previous results regarding the shape of the spectrum and the variation with laser irradiance were corroborated in the present experiment. We also measured the approximate ionization distribution both with and without the contribution from the hump. The relative intensities in the $3d$-$4f$ transitions from the different ionization stages are shown in Table IV. The experimental values represent the sum over all the identified transitions. The intensities were scaled according to the average number of electrons in the ground state ($\frac{1}{10}$Ni:$\frac{1}{9}$Co:$\frac{1}{8}$Fe). The relative intensities of the $3d$-$4f$ transitions were compared with the ionization distribution predicted by a CR model (Tables IV and V). The values shown in Table IV were calculated for the experimental plasma conditions indicated in the opacity estimate below. Table V lists the percent ion abundances as a function of temperature and density. The distributions given in Tables IV and V are for time-integrated plasma parameters. By starting the calculation with an arbitrary distribution and allowing the distribution to relax to equilibrium while keeping the plasma parameters fixed, we found that the time scale for ionization equilibrium was 50 psec. For typical velocities ($\sim 3\times 10^7$ cm/sec), plasma ions move about 15 μm during 50 psec. Thus the ionization distribution should reflect the plasma conditions in each spatial region.

The results from the CR model agree to within one ionization state with the experimental line intensity ratios. However, the CR results do not agree with the experiment when the contribution from the quasicontinuum hump is included. Table IV shows that the Ni-like to Co-like ratio is reduced to 0.13–0.18 when the hump is included. According to the CR model this is not possible unless the Fe-like radiation is much stronger than the Co-like radiation, which is not the case experimentally. This is true independent of the plasma parameters and the computational details (i.e., dielectronic recombination rate or number of high-n levels included). This agrees with our expectation that the distribution of ionization states should be relatively broad, since there is no physical reason for the distribution to "pile up" in the Co-like state. Our conclusion is that the hump originates from transitions in some other ionization state, possibly from satellites originating from doubly excited levels in the lower ionization state.

One effect which could influence this result is opacity. From previous experiments[14] we expect $n_e \sim 6\times 0^{21}$ cm^{-3}, $T_e \sim 500$ eV for the high-irradiance shot, and $n_e \sim 1\times 10^{21}$ cm^{-3}, $T_e \sim 400$ eV for the low-irradiance shot. The line ratios from aluminum emission observed in the present experiment agree qualitatively with the previous result, but the K-shell lines observed in these spectra were insuf-

TABLE III. Identifications of Fe-like europium. The theoretical wavelengths were shifted upward by 13 mÅ. The levels are labeled in *j-j* coupling, with the indicated purity.

				Ground state $(3d^r_{3/2})_s(3d^t_{5/2})_u$					Upper state $[(3d^r_{3/2})_s(3d^t_{5/2})_u]_v 4f_w$								
Line	Expt. λ	Theor. λ	gf	r	s	t	u	J	r	s	t	u	v	w	J'	Purity
30	8.538	8.532	3.3	3	3/2	5	5	1	2	0	5	5/2	5/2	5/2	2	0.21
29	8.531	8.529	5.5	2	0	6	0	0	1	3/2	6	0	3/2	5/2	1	0.52
28	8.522	8.518	4.3	3	3/2	5	5/2	1	2	2	5	5/2	5/2	5/2	5	0.31
27	8.512	8.511	1.5	3	3/2	5	5/2	3	2	2	5	5/2	7/2	5/2	3	0.12
26	8.509	8.505	3.0	3	3/2	5	5/2	2	2	2	5	5/2	7/2	5/2	1	0.35
25	8.502	8.501	6.0	2	2	6	0	2	1	3/2	6	0	3/2	5/2	2	0.76
24	8.492	8.499	3.6	3	3/2	5	5/2	2	2	2	5	5/2	7/2	5/2	2	0.63
23	8.492	8.498	10.4	3	3/2	5	5/2	4	2	2	5	5/2	9/2	5/2	4	0.41
22	8.487	8.492	3.9	4	0	4	4	4	3	3/2	4	0	3/2	5/2	3	0.37
21	8.483	8.480	3.6	4	0	4	4	4	3	3/2	4	0	3/2	5/2	3	0.27
20	8.474	8.475	4.1	4	0	4	2	2	3	3/2	4	2	5/2	5/2	2	0.23
19	8.470	8.473	8.2	3	3/2	5	5/2	2	2	2	5	5/2	7/2	5/2	3	0.31
18	8.470	8.472	3.2	3	3/2	5	5/2	3	2	2	5	5/2	9/2	5/2	3	0.29
17	8.470	8.472	3.0	4	0	4	2	2	3	3/2	4	2	7/2	5/2	1	0.40
16	8.464	8.460	13.9	4	0	4	4	4	3	3/2	4	4	11/2	7/2	4	0.30
15	8.459	8.464	1.0	3	3/2	5	5/2	3	2	0	5	5/2	5/2	5/2	2	0.21
14	8.459	8.463	0.9	4	0	4	2	2	3	3/2	4	2	5/2	5/2	2	0.24
13	8.459	8.462	1.7	4	0	4	4	4	3	3/2	4	4	11/2	7/2	4	0.30
12	8.459	8.461	5.7	4	0	4	2	2	3	3/2	4	2	1/2	5/2	3	0.28
11	8.451	8.455	3.7	4	0	4	4	4	3	3/2	4	2	5/2	7/2	5	0.29
10	8.451	8.453	3.3	3	3/2	5	5/2	3	2	2	5	5/2	9/2	5/2	3	0.41
9	8.451	8.452	16.2	3	3/2	5	5/2	3	2	2	5	5/2	5/2	5/2	4	0.29
8	8.451	8.451	2.5	3	3/2	5	5/2	1	2	0	5	5/2	5/2	5/2	1	0.25
7	8.451	8.450	14.9	4	0	4	4	4	2	2	5	5/2	5/2	5/2	5	0.14
6	8.451	8.450	3.2	4	0	4	0	0	3	3/2	4	0	3/2	5/2	1	0.56
5	8.451	8.448	13.8	2	2	6	0	2	1	3/2	6	0	3/2	5/2	3	0.72
4	8.443	8.441	4.7	3	3/2	5	5/2	4	2	0	5	5/2	5/2	5/2	4	0.61
3	8.443	8.439	2.0	4	0	4	2	2	2	2	5	5/2	9/2	7/2	3	0.26
2	8.443	8.439	2.0	3	3/2	5	5/2	1	2	0	5	5/2	5/2	5/2	2	0.62
1	8.428	8.432	18.3	3	3/2	5	5/2	4	2	0	5	5/2	5/2	5/2	5	0.45

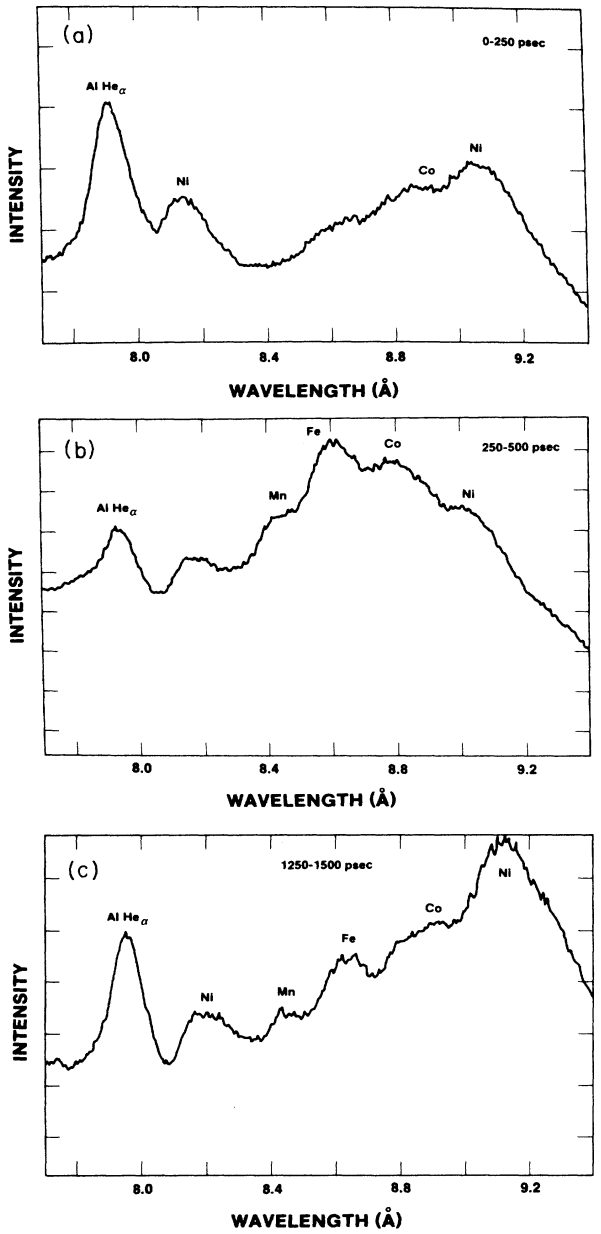

FIG. 4. A sequence of tracings from the streaked spectrograph. The indicated times are relative to an arbitrary zero.

ficient to provide a definitive measurement. These values imply an optical depth of 12 (assuming a Doppler profile) for the strongest Ni-like line in the high-irradiance spectrum and 2 in the low-irradiance spectrum. The Co-like and Fe-like lines are all optically thin.

Since the $4f$ levels are very close together in energy, we can assume they are in local thermal equilibrium. Then the experimental intensity ratio $R=3d^9_{3/2}4f_{5/2}/3d^9_{5/2}4f_{7/2}$ should be the same as the ratio of the gf's (6.1). For the high-irradiance case $R=3.3$. This indicates a possible opacity correction of about 2 for the $3d^9_{3/2}4f_{5/2}$ line, since the $3d^9_{5/2}4f_{7/2}$ line is approximately thin. However, $R=3$ for the low-irradiance shot as well, where we expect n_e and the optical depth are lower. Thus opacity may be negligible even in the high-irradiance case. In any case, the initial effect of opacity is to redistribute the photons into a broader line. This does not affect our intensity measurements since we measure the area under the line.

The experimental results were also compared with a two-dimensional LASNEX simulation (a one-dimensional simulation was found to result in temperatures which were too high and an average ionization state of Cr-like). A discussion of the atomic physics and radiation model in LASNEX can be found in Ref. 15. For the low-irradiance laser pulse, LASNEX predicts $T_e=413$ eV, $n_e=8.5\times10^{20}$ cm^{-3}, and $\overline{Z}=30$ (Zn-like; $\overline{Z}$ is the average ionization state) 0.5 nsec before the peak of the laser pulse, and it predicts $T_e=618$ eV, $n_e=4.5\times10^{20}$ cm^{-3}, and $\overline{Z}=28$ (Ni-like) at the peak. At later times the europium portion of the plasma has moved away from the target surface. Work is now proceeding to carry out a two-dimensional XRASER[16] calculation, using the two-dimensional LASNEX plasma parameters, to obtain the $n=4$ to $n=3$ time- and space-dependent emission spectrum. This would eliminate the need for assuming that the $3d$-$4f$ intensity ratios reflect the ionization distribution, since we could make a direct comparison between the theoretical and experimental spectrum.

In summary, we have identified new transitions in Ni-like, Co-like, and Fe-like europium. For the present irradiation conditions Co-like is the dominant ionization state, with Ni-like increasing at lower laser irradiance. The latter observation could be important, since Ni-like europium has been suggested as an x-ray laser candidate.[17] The predictions of LASNEX and the CR model are

TABLE IV. Relative $3d$-$4f$ intensities of Ni-, Co-, and Fe-like europium. The experimental intensities correspond to the tracings shown in Fig. 1(b) (average over 100 μm of plasma). The plasma parameters used for the CR calculations were $n_e\sim6\times10^{21}$ cm^{-3}, $T_e\sim500$ eV for the high-irradiance case, and $n_e\sim1\times10^{21}$ cm^{-3}, $T_e\sim400$ eV for low irradiance.

	Relative experimental intensity								
	Lines only			Lines plus continuum			Predictions of CR model		
	Ni	Co	Fe	Ni	Co	Fe	Ni	Co	Fe
Low laser intensity	0.66	1.00	0.65	0.18	1.00	0.22	1.00	0.38	0.07
High laser intensity	0.40	1.00	0.58	0.13	1.00	0.66	0.43	1.00	0.80

TABLE V. Ionization distribution predicted by the CR model for two different electron densities. The numbers below each ionization state indicate the percent composition.

	$n_e = 6\times10^{21}$ cm^{-3}				$n_e = 1\times10^{21}$ cm^{-3}			
T_e (eV)	Cu	Ni	Co	Fe	Cu	Ni	Co	Fe
400	26	11	6	1	13	2	0.1	
500	13	18	32	20	33	15	4	0.4
600	2	6	22	35	29	28	18	6
700	0.2	1	7	23	14	23	30	19
800		0.2	2	9	4	11	24	28

close to the experimental result. When the hump is included in the measurement of the $3d$-$4f$ intensity, the ionization distribution disagrees with theory. This is qualitative evidence that the origin of the hump is transitions from other ionization states, possibly satellites from doubly excited levels. Therefore, to determine the ionization distribution from the $3d$-$4f$ transitions, it is necessary to resolve the lines. It is not sufficient to resolve only the arrays, although for other configurations (e.g., $3d$-$5f$) the array alone might be enough. Improved experiments could address this issue by using a framing camera for simultaneous space and time resolution and appropriate K-shell impurities added for diagnostics. This would also be useful for determining the suitability of such a plasma as an x-ray laser source.

ACKNOWLEDGMENTS

Useful discussions on the subject of ionization distribution with R. J. Fortner and R. E. Stewart are gratefully acknowledged. We also thank J. Swain and P. Salone for assistance in performing the experiments.

[1]P. G. Burkhalter, D. J. Nagel, and R. R. Whitlock, Phys. Rev. A **9**, 2331 (1974).

[2]M. Klapisch, A. Bar-Shalom, P. Mandelbaum, J. L. Schwob, A. Zigler, H. Zmora, and S. Jackel, Phys. Lett. **79A**, 67 (1980).

[3]A. Zigler, H. Zmora, N. Spector, M. Klapisch, J. L. Schwob, and A. Bar-Shalom, J. Opt. Soc. Am. **70**, 129 (1980).

[4]A. Zigler, H. Zmora, N. Spector, M. Klapisch, J. L. Schwob, and A. Bar-Shalom, Phys. Lett. **75A**, 343 (1980).

[5]P. Mandelbaum, M. Klapisch, A. Bar-Shalom, J. L. Schwob, and A. Zigler, Phys. Scr. **27**, 39 (1983).

[6]M. Busquet, D. Pain, J. Bauche, and E. Luc-Koenig, Phys. Scr. **31**, 137 (1985).

[7]M. Klapisch, E. Meroz, P. Mandelbaum, A. Zigler, C. Bauche-Arnoult, and J. Bauche, Phys. Rev. A **25**, 2391 (1982).

[8]P. Audebert, J. C. Gauthier, J.-P. Geindre, C. Chenais-Popovics, C. Bauche-Arnoult, J. Bauche, M. Klapisch, E. Luc-Koenig, and J.-F. Wyart, Phys. Rev. A **32**, 409 (1985).

[9]M. J. Herbst, P. G. Burkhalter, J. Grun, R. R. Whitlock, and M. Fink, Rev. Sci. Instrum. **53**, 1418 (1982).

[10]P. G. Burkhalter, M. J. Herbst, D. Duston, J. Gardner, M. Emery, R. R. Whitlock, J. Grun, J. P. Apruzese, and J. Davis, Phys. Fluids **26**, 3650 (1983).

[11]P. D. Rockett, C. R. Bird, C. J. Hailey, D. Sullivan, D. B. Brown, and P. G. Burkhalter, Appl. Opt. **24**, 2536 (1985).

[12]J. V. Gilfrich, D. B. Brown, and P. G. Burkhalter, Appl. Spectrosc. **26**, 3650 (1983).

[13]J. H. Scofield, Phys. Rev. A **9**, 1041 (1974).

[14]J. Bailey, R. E. Stewart, J. D. Kilkenny, R. S. Walling, T. Phillips, R. J. Fortner, and R. W. Lee, J. Phys. B **19**, 2639 (1986).

[15]G. B. Zimmerman, Lawrence Livermore National Laboratory Report No. UCRL-74811, 1973 (unpublished); P. D. Nielson and G. B. Zimmerman, Lawrence Livermore National Laboratory Report No. UCRL-53123, 1981 (unpublished).

[16]P. G. Hagelstein, Ph.D. thesis, Massachusetts Institute of Technology, 1981; Lawrence Livermore National Laboratory Report No. UCRL-53100, 1981 (unpublished).

[17]S. Maxon, P. Hagelstein, J. Scofield, and Y. Lee, J. Appl. Phys. **59**, 293 (1986).